

HIGH-SPEED TRANSMISSION
SHADOWGRAPHIC AND DYNAMIC
PHOTOELASTICITY STUDY OF STRESS WAVE
AND IMPACT DAMAGE PROPAGATION IN
TRANSPARENT MATERIALS AND LAMINATES
USING THE EDGE-ON IMPACT (EOI) METHOD

Elmar Strassburger, Ernst-Mach-Institut (EMI),
Efringen-Kirchen, Germany
Parimal Patel, James W. McCauley, Army Research
Laboratory, APG, MD,
Christopher Kovalchick, K.T. Ramesh, Johns
Hopkins University and Douglas W. Templeton, US
Army TARDEC, Warren, MI

ABSTRACT

Operation Iraqi Freedom has clearly demonstrated the criticality of transparent armor in many army systems. As the threats have escalated and become more varied, the challenges for rapidly developing optimized threat specific transparent armor packages have become extremely complex. In order to accelerate the development of validated design and predictive performance models, the Army Research Laboratory, the U.S. Army Tank Automotive Research Development and Engineering Center, and the Material Center of Excellence at Johns Hopkins University have entered into a collaboration with The Ernst-Mach Institute (EMI) of Efringen-Kirchen, Germany. The unique, fully instrumented Edge-on Impact facility at EMI, modified for dynamic photoelasticity, is being used to quantify stress wave propagation, damage nucleation and propagation during high velocity impacts. Summarized in this paper are a selection of results on monolithic and laminated glass (Starphire™) and AION, a polycrystalline transparent ceramic. Crack, damage and stress wave velocities have been determined directly. In addition, the stress wave and damage retardation by various thickness bonding interfaces has been measured: for a 5.08 mm interlayer, a delay of 1.7 μs was determined. A computational model was constructed using ABAQUS Explicit to simulate the elastic wave propagation within AION. The simulations show that the damaged region observed in the experiments corresponds essentially to the region that has observed shear as a result of the wave propagation. These results are a critical tool to corroborate and refine existing materials and transparent armor package models by providing insight and critical data into the role of different materials and interfaces that can eventually guide materials and laminate design.

EXPERIMENTAL SET-UP

An Edge-on Impact (EOI) test method coupled with a high speed Cranz-Schardin camera, with 0.10 μs resolution, has been developed at the Fraunhofer-Institute for High-Speed Dynamics, EMI, to visualize damage propagation and dynamic fracture in structural ceramics. Most work in the past has been carried out in a reflection mode from the surface of impacted ceramics. In the current study, the test was reconfigured to photograph the propagation of damage in the transmission mode using shadowgraphs. In addition to plane light observations, the test set up has been modified to visualize the stress waves using dynamic photoelasticity techniques. Figure 1 is a schematic of the Edge-on Impact test with the added crossed polarizers; Figure 2 illustrates an exploded view of the impactor/sample interaction.

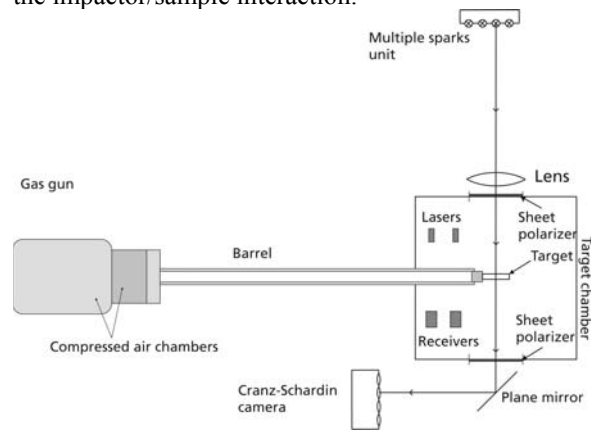


Fig. 1: EOI Test Set-up with 1 Cranz-Schardin camera

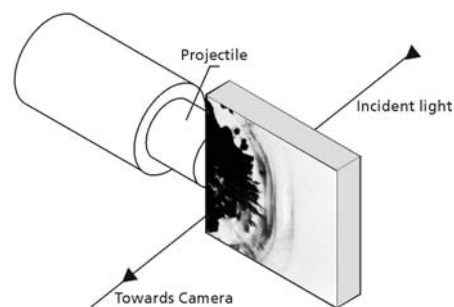


Fig. 2: Test sample set up for shadowgraphs

Both steel solid cylinder and spherical impactors have been used at velocities from 270- 925 m/s on 100x100x10 mm plates. Four different materials and laminates of the glass materials were produced, tested, and analyzed: aluminum oxynitride spinel (ALON™), fused silica, Starphire™, a soda-lime-

Report Documentation Page

*Form Approved
OMB No. 0704-0188*

Public reporting burden for the collection of information is estimated to average 1 hour per response, including the time for reviewing instructions, searching existing data sources, gathering and maintaining the data needed, and completing and reviewing the collection of information. Send comments regarding this burden estimate or any other aspect of this collection of information, including suggestions for reducing this burden, to Washington Headquarters Services, Directorate for Information Operations and Reports, 1215 Jefferson Davis Highway, Suite 1204, Arlington VA 22202-4302. Respondents should be aware that notwithstanding any other provision of law, no person shall be subject to a penalty for failing to comply with a collection of information if it does not display a currently valid OMB control number.

1. REPORT DATE 01 NOV 2006	2. REPORT TYPE N/A	3. DATES COVERED -	
4. TITLE AND SUBTITLE High-Speed Transmission Shadowgraphic and Dynamic Photoelasticity Study of Stress Wave and Impact Damage Propagation in Transparent Materials and Laminates		5a. CONTRACT NUMBER	
		5b. GRANT NUMBER	
		5c. PROGRAM ELEMENT NUMBER	
6. AUTHOR(S)		5d. PROJECT NUMBER	
		5e. TASK NUMBER	
		5f. WORK UNIT NUMBER	
7. PERFORMING ORGANIZATION NAME(S) AND ADDRESS(ES) Efringen-Kirchen, Germany		8. PERFORMING ORGANIZATION REPORT NUMBER	
9. SPONSORING/MONITORING AGENCY NAME(S) AND ADDRESS(ES)		10. SPONSOR/MONITOR'S ACRONYM(S)	
		11. SPONSOR/MONITOR'S REPORT NUMBER(S)	
12. DISTRIBUTION/AVAILABILITY STATEMENT Approved for public release, distribution unlimited			
13. SUPPLEMENTARY NOTES See also ADM002075., The original document contains color images.			
14. ABSTRACT			
15. SUBJECT TERMS			
16. SECURITY CLASSIFICATION OF:			17. LIMITATION OF ABSTRACT
a. REPORT unclassified	b. ABSTRACT unclassified	c. THIS PAGE unclassified	UU
			18. NUMBER OF PAGES 29
			19a. NAME OF RESPONSIBLE PERSON

silica glass, and borofloat glass. Once the baseline glass materials were tested and analyzed, multi-component glass laminates were produced and tested at 350 - 400 m/s. The data collected from the EOI test consists of a series of 20 photographs as a function of time, typically at 0.25 - 2 μs intervals. Pairs of impact tests at approximately equivalent velocities are carried out in plane and crossed polarized light to correlate the dynamic fracture with the associated stress fields. Detailed graphs are then created plotting crack, damage (failure wave) and compression and shear stress wave velocities; exact measurements of bonding layer stress wave and damage zone dwell times are also determined.

BASELINE RESULTS WITH GLASS

Experiments performed in plane light show the evolution of damage and material failure, while the photoelastic visualization illustrates the stress wave propagation as a function of time. Figure 3 shows a selection of two shadowgraphs (top) and corresponding crossed polarizers photographs (bottom) of a baseline test with Starphire™ glass, impacted by a spherical steel projectile of 16 mm diameter at 440 m/s. The shadowgraphs show a crack front growing from the impacted edge of the specimen. Only one crack center can be observed close to the upper edge of the specimen. The crossed polarizers photographs illustrate the propagation of the longitudinal and the transversal stress waves. Release waves due to reflections at the upper and lower edge can also be recognized. Note that damage appears dark on the shadowgraphs and the zones with stress birefringence are exhibited as bright zones in the crossed polarizers photographs. The path-time histories of the longitudinal and transversal waves and the crack front propagation are depicted in Figure 4.

Figure 5 shows a selection of two shadowgraphs along with the corresponding crossed polarizers photographs of the baseline tests with the cylindrical projectile. A coherent damage zone is growing from the impacted edge, preceded by a zone with separated crack centers, initiated by the stress waves. The path-time histories of the stress waves and the damage propagation are depicted in Figure 6. It can be recognized that the stress wave front appears more advanced and exhibits a different curvature in the crossed polarizers view. This seeming discrepancy can be explained by the different sensitivities that the different optical techniques employed exhibit with respect to the stress level that can be visualized. In a shadowgraph image the light intensity depends on the

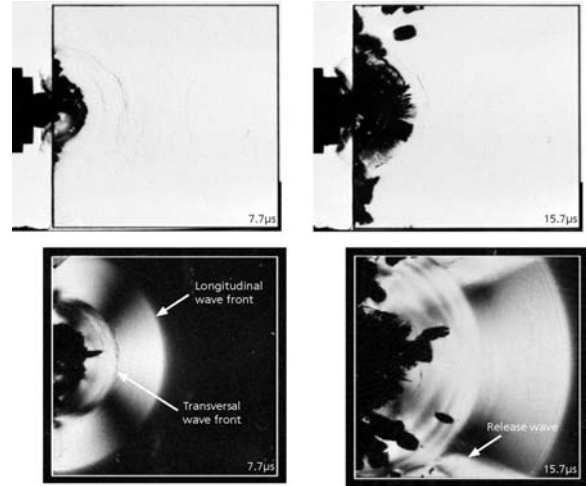


Fig. 3: Selection of two shadowgraphs (top) and corresponding crossed polarizers photographs (bottom) from impact on Starphire glass with steel ball at 440 m/s.

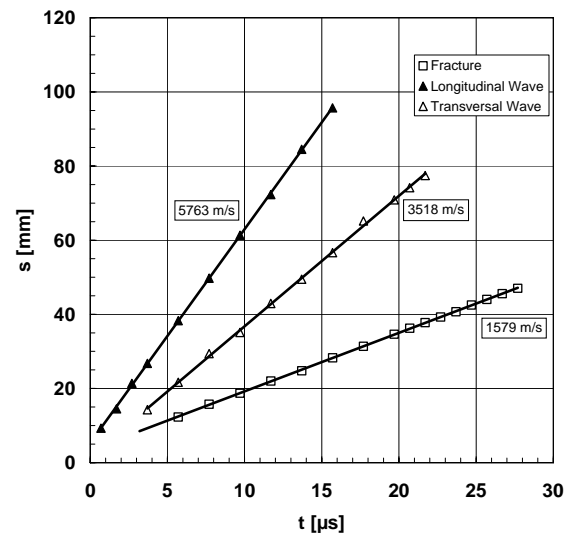


Fig. 4: Path-time history of wave and crack propagation in Starphire glass depicted in figure 3.

second spatial derivative $\partial^2 n / \partial x^2$ of the refractive index, whereas in the crossed polarizers set-up the intensity of the transmitted light depends on the photo-elastic properties of the material. Therefore, it is possible that the first visible wave front in the shadowgraph configuration appears at a different position than the forefront of the stress wave, visible in the crossed polarizers set-up. Both techniques can visualize different parts of the same stress wave.

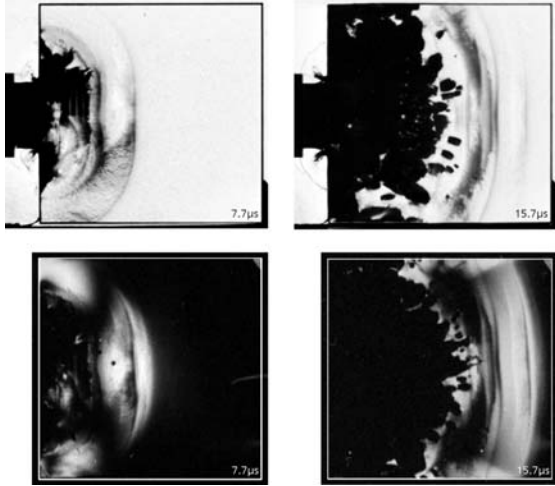


Fig. 5: Selection of two shadowgraphs and corresponding crossed polarizers photographs from impact on Starphire glass with steel cylinder at 390 m/s

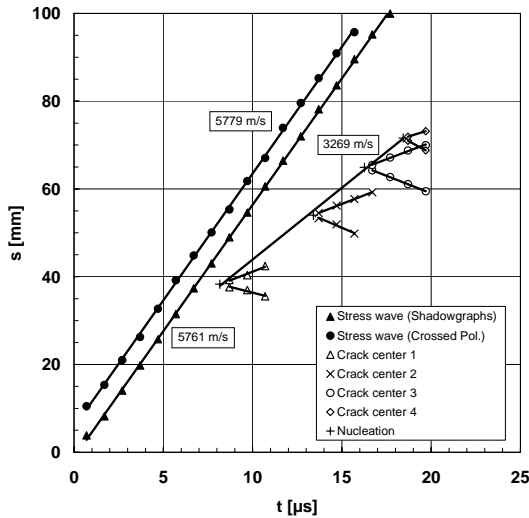
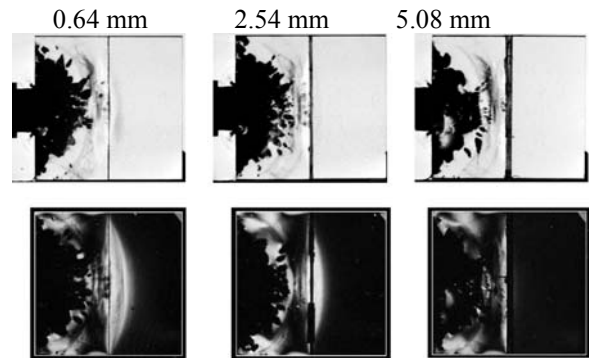


Fig. 6: Path-time history of wave and damage propagation in Starphire glass depicted in figure 5.

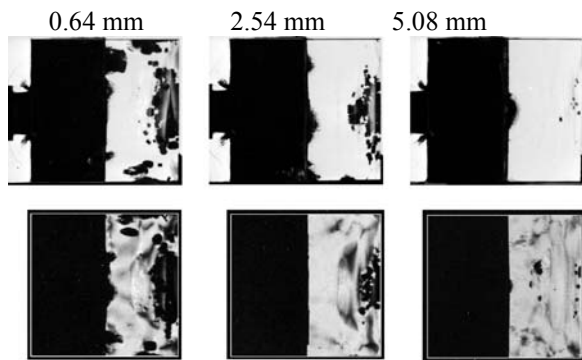
The expansion of four crack centers at the front of the damage zone was also analyzed (Fig. 6) and the slope of the straight line through the nucleation sites, which is denoted damage velocity v_D , was 3269 m/s, which means, that the damage velocity is close to the transversal wave velocity. This result is in agreement with the observations made with other types of glass in previous studies [1, 2].

GLASS LAMINATES

The influence of a polyurethane (PU) bonding layer on wave and damage propagation was examined with cylindrical projectiles only. Four pairs of tests with specimens consisting of two parts of the dimensions 50 mm x 100 mm x 9.5 mm were conducted in order to examine the influence of interlayer thickness. Starphire specimens with bonding layers of thickness 0.64 mm, 1.27 mm, 2.54 mm and 5.08 mm were examined. The influence of two PU interlayers (2.54 mm) was also tested with specimens that were built of three parts of the dimensions 30 mm x 100 mm x 9.5 mm. Figure 7 illustrates a comparison of wave propagation and damage in Starphire specimens with bonding layers of thickness 0.64 mm, 2.54 mm and 5.08 mm. The impact velocity was 380 ± 5 m/s in all tests. The upper line of pictures shows the shadowgraphs, while the corresponding crossed polarizers photographs are presented in the lower line of pictures, respectively. Figure 7a illustrates the specimens at 10.7 μ s and Figure 7b at 23.7 μ s after projectile impact. The shadowgraphs at 10.7 μ s show that the first glass layer (left part of specimen) is damaged through the coherent fracture front growing from the impacted edge and through the nucleation of crack centers, initiated by the longitudinal stress waves. At that time, no damage can be recognized in the second glass layer (right part of specimen). The crossed polarizers photographs demonstrate, that the first longitudinal stress pulse has not yet crossed the thickest glue interlayer (right), whereas the stress wave is clearly visible in the right half of the specimens with the thinner glue interlayer.



a.) 10.7 μ s



b.) 23.7 μ s

Fig. 7: Starphire laminates with interlayer of different thickness impacted by steel cylinder at 380 m/s

After 23.7 μ s (Figure 7b) the compressive stress pulse has already been reflected as a tensile wave at the rear edge of the specimens in all three cases. The shadowgraphs illustrate that damage in the second glass layer is mainly due to the tensile wave and starts from the rear edge of the specimen. In the case of the thickest glue interlayer only little damage was observed in the second glass layer. The wave propagation in the specimens was analyzed and the path-time history for the case with the 5.08 mm bonding layer is presented in Figure 8.

When the waves hit the interlayer one part is reflected while the other part is transmitted into the second glass layer. Due to the low acoustic impedance of the interlayer compared to the glass, the amplitude of the stress pulses is attenuated considerably. The low wave velocity in the interlayer effects a time delay of 1.7 μ s compared to the unperturbed propagation through the glass. The delay times measured in all tests were plotted in a delay time versus bonding layer thickness diagram (Figure 9). Linear regression of the data yielded an average delay time of 0.33 μ s/mm. This is in good agreement with the calculated value based on a longitudinal wave velocity $c_L = 5770$ m/s for Starphire glass and $c_L \approx 2000$ m/s for the polyurethane [3]. The effect of two bonding layers of 2.54 mm thickness is demonstrated in Figure 10 which shows a selection of four shadowgraphs and corresponding crossed polarizers photographs in the time interval from 6 – 25 μ s after impact of a steel cylinder at about 400 m/s. The first layer of glass was completely damaged within the first 15 μ s. Damage could be recognized in the second layer after 16 μ s, when the first crack centers became visible which were initiated by the

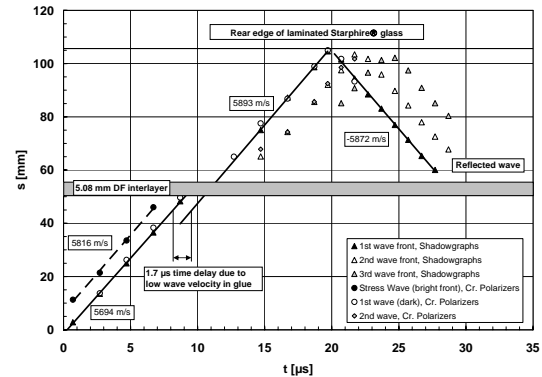


Fig. 8: Path-time history of wave propagation in specimens with one 5.08 mm polyurethane (DF) interlayer

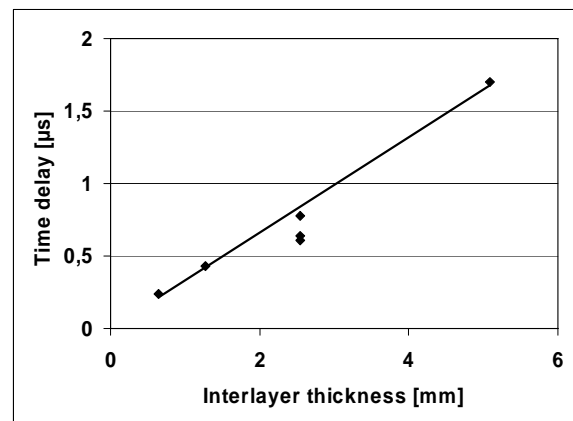


Figure 9. Interlayer bonding delay time versus bonding layer thickness.

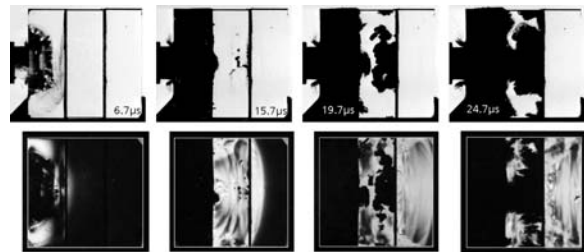


Fig. 10: Selection of four shadowgraphs and corresponding crossed polarizers photographs; Starphire specimen with two PU bonding layers; Impact velocity 400 m/s

reflection of the compression wave at the interface between the second glass and the second bonding layer. No damage was observed in the third glass layer during the time interval of observation.

AION

Recent progress in material technology has also made available aluminum oxynitride (AION) as a polycrystalline ceramic that fulfills the requirements of transparency and requisite mechanical properties [4]. AION has a cubic crystal structure (Fd3m) that can be processed to transparency in a polycrystalline microstructure. It differs from glasses which do not have any periodic crystalline order, but is akin to polycrystalline opaque ceramics such as aluminum oxide. The grain size is typically 150 – 250 μm on average. The density is typically 3.67 g/cm^3 , but will vary slightly depending on the composition and porosity. Figure 11 shows a selection of four shadowgraphs along with the corresponding photographs in the crossed polarizers arrangement for tests at 380 m/s nominal impact velocity, using a solid cylinder impactor.

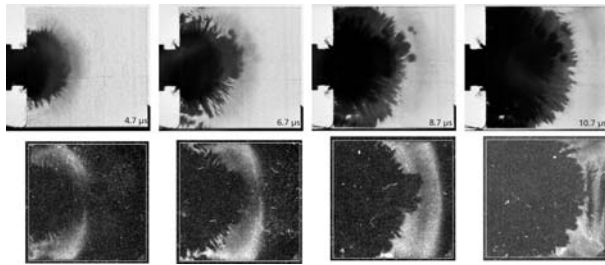


Fig. 11: Selection of four shadowgraphs and corresponding crossed polarizers photographs of AION specimen; impact velocity 380 m/s; solid cylinder.

The high-speed photographs show rapidly growing darkened to opaque regions, which reflect changes in the optical transmission due to pressure induced refractive index changes, damage and fractured zones within the specimen. In addition, the nucleation of crack centers ahead of the crack front is clearly visible 8.7 μs after impact. In contrast to the shadowgraphs, where a wave front is not discernible, the crossed polarizers configuration reveals an approximately semicircular wave front which is a little further advanced compared to the damage front visible in the shadowgraphs at the same time. From the crossed polarizers photographs a wave front velocity of 9367 m/s was determined. The coherent damage/fracture front initiated at the impacted edge of the specimen propagated at an average velocity of 8381 m/s. The observed crack centers were generated in the interior of the specimens. This was validated with a test on an aluminum coated AION specimen to mimic the observations from previous work on opaque ceramic [5].

Figure 12 illustrates the distinct change in damage morphology and propagation (top row) and the nature of the stress waves (bottom row) when a spherical impactor is used instead of a solid cylinder of much more mass.

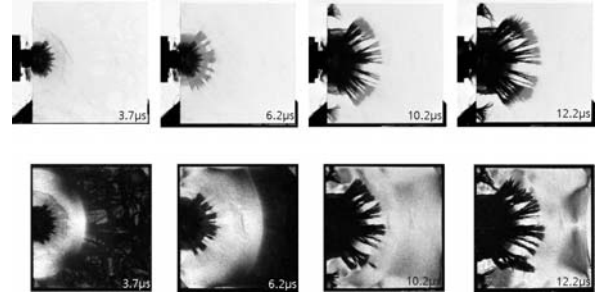


Figure 12. Spherical steel impactor on AION at 429 m/s: top row is plane light, bottom row is crossed polarized light.

MODELLING

We have performed computational simulations of the elastic wave propagation within the Edge-on Impact (EOI) experiments on AION ceramic specimens [5]. In the experiments, the EOI technique was coupled with a Cranz-Schardin high-speed camera to enable direct visualization of damage development and wave propagation through the solid (both with and without crossed polarizers). A computational model was constructed using ABAQUS Explicit to simulate the elastic wave propagation within the experiment. Since the experiment provides snapshots of the deformation and the stress state at specific times, the simulation results provide snapshots at identical times for comparison. The computational model was fully 3-dimensional, so that longitudinal and shear waves, surface waves and plate waves could all be captured.

The computational results show the observed propagation of the longitudinal wave in the specimen as a result of the impact, as well as the subsequent edge unloading. The simulations also show that the damaged region observed in the experiments corresponds essentially to the region that has observed shear as a result of the wave propagation (Figure 13). The character of the damage itself, and its kinetics, can of course NOT be captured with this elastic simulation. However, the correlation of the damage propagation speed with the shear information is a useful correlation. In later work, we will explore the development of damage within the specimen using computational damage models.

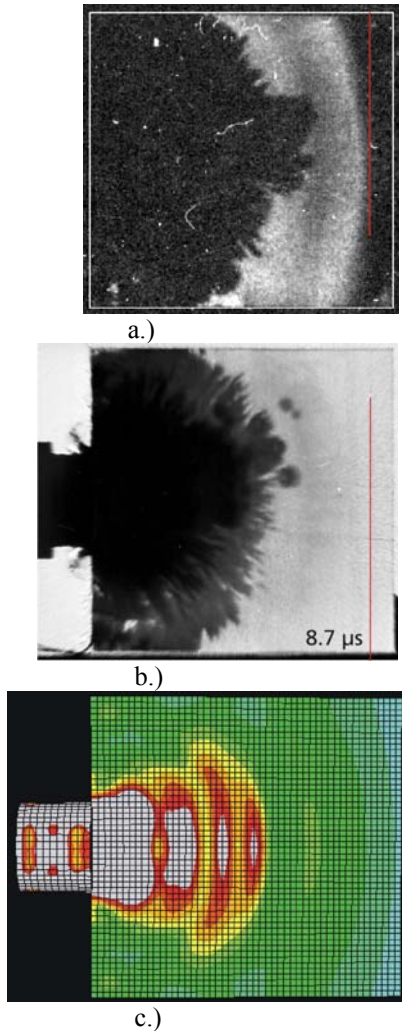


Figure 13. Comparison of experimental images (showing damage and stress waves) with computed equivalent shear stress state (from elasticity) at identical times ($8.7 \mu\text{s}$) after impact at 381 m/s : a.) crossed polarizers – stress wave; b.) plane light – damage; c.) model calculation

CONCLUSION

The edge-on Impact test method was applied in order to visualize wave and damage propagation in materials for transparent armor. The influence of bonding layer thickness on damage evolution in Starphire glass laminates was examined. The high resolution of the high-speed photographs allowed for the determination of the stress wave time delay during the transition through the bonding layers. It is expected that the capabilities of the experimental method help with the development of damage models and that the combination of experimental and computational modelling results can eventually guide materials and laminates design.

REFERENCES

- [1] E. Strassburger, H. Senf, “Experimental Investigations of Wave and Fracture Phenomena in Impacted Ceramics and Glasses”, U.S. Army Research Laboratory contractor report ARL-CR-214, 1995
- [2] E. Strassburger, P. Patel, J.W. McCauley, D.W. Templeton: “High-Speed Photographic Study of Wave and Fracture Propagation in Fused Silica”; pp. 761-768, Proc. 22nd Int. Symposium on Ballistics, Vancouver, BC Canada, November 14-18, 2005
- [3] Y.M. Gupta: “High Strain-Rate Shear Deformation of a Polyurethane Elastomer Subjected to Impact Loading”; Polymer Engineering and Science, 1984, Vol. 24, No. 11
- [4] P. J. Patel, G. A. Gilde: “Transparent Armor Materials: Needs and Requirements”; Ceramic Transactions Vol. 134, pp. 573-586, Proc. of the Ceramic Armor Materials by Design Symposium, Pac Rim IV International Conference on Advanced Ceramics and Glass, November 4-8, 2001, Wailea, Maui, Hawaii
- [5] E. Strassburger, P. Patel, J.W. McCauley, D.W. Templeton: “Visualization of Wave Propagation and Impact Damage in a Polycrystalline Transparent Ceramic – AlON”; pp. 769-776, Proc. 22nd Int. Symposium on Ballistics, Vancouver, BC Canada, November 14, 2005.

High-Speed Transmission Shadowgraphic and Dynamic Photoelasticity Study of Stress Wave and Impact Damage Propagation in Transparent Materials and Laminates

Elmar Strassburger, Martin O. Steinhauser
Ernst-Mach-Institut (EMI), Germany

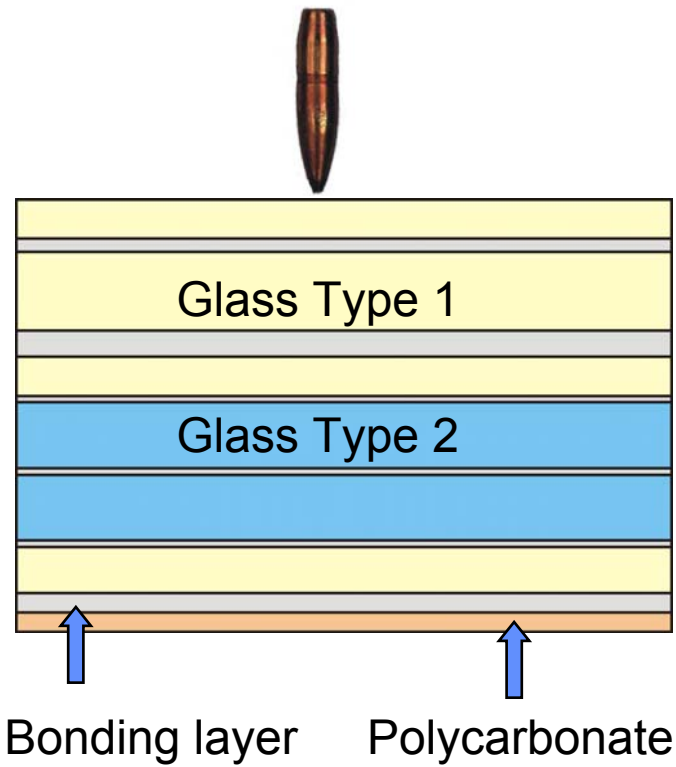
Parimal Patel, James W. McCauley
Army Research Laboratory, APG, MD

Christopher Kovalchick, K.T. Ramesh
Johns Hopkins University

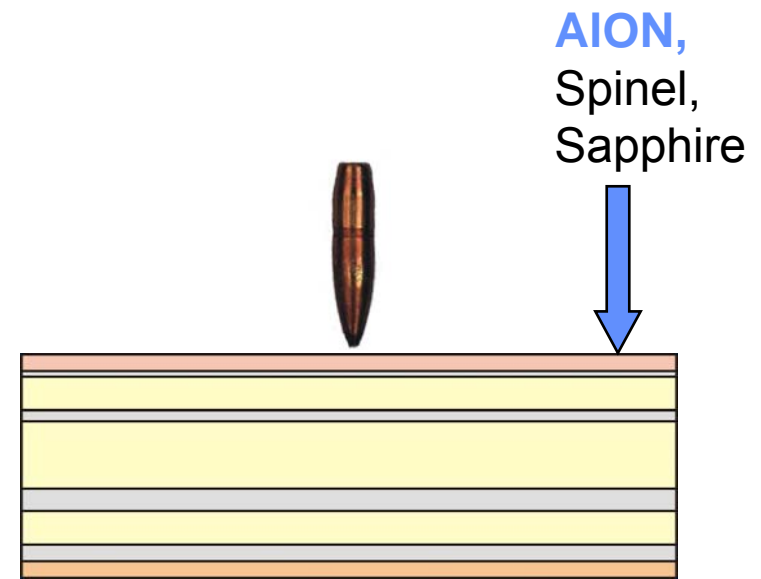
Douglas W. Templeton
US Army TARDEC, Warren, MI

Introduction

Conventional Transparent Armor



Ceramic Faced Transparent Armor



Objective of the study

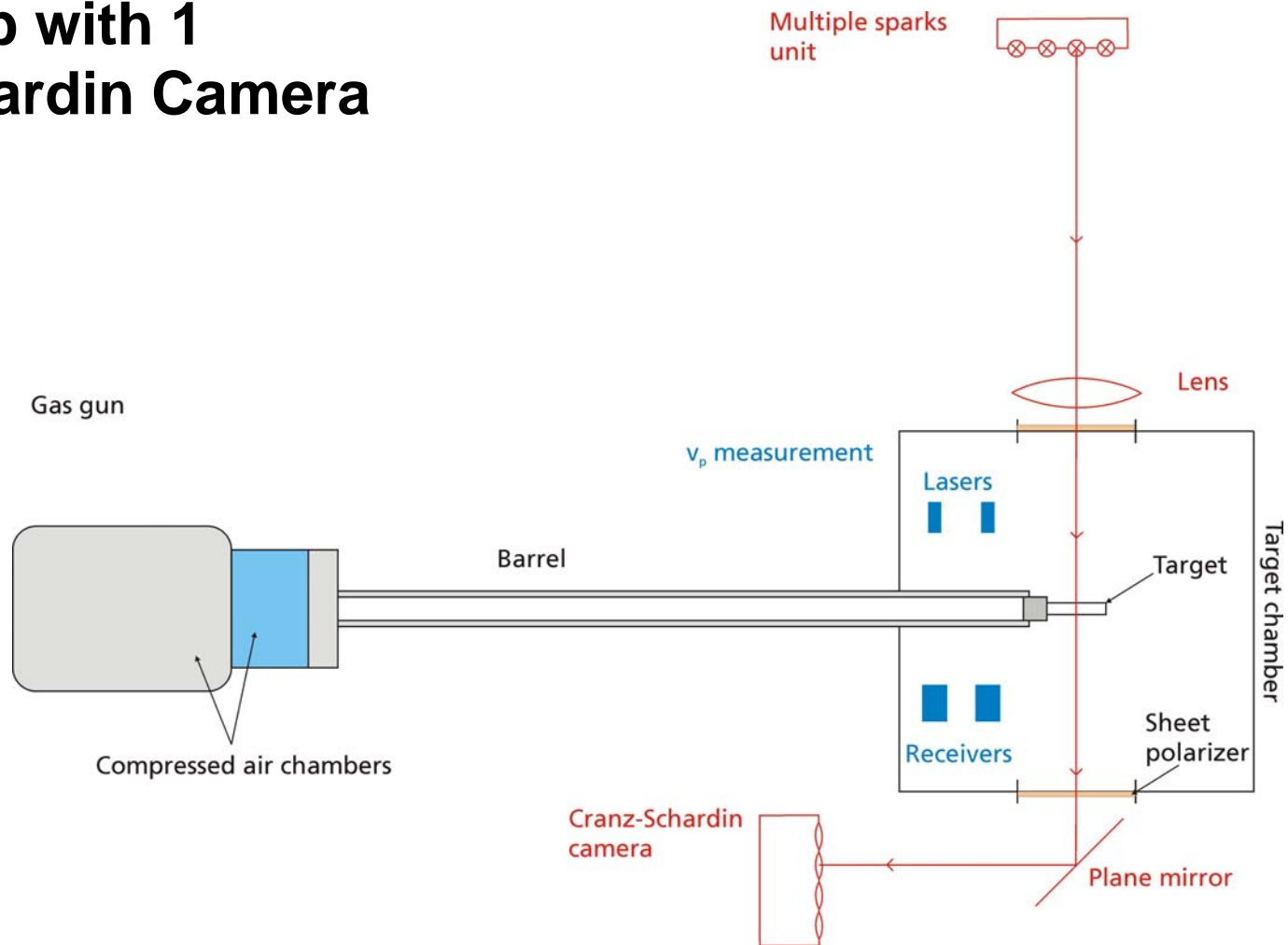
- Provide data and insight into the role of different materials and interfaces
- Validate and improve material and damage models for the single materials and transparent laminates
- Guidance for the design of transparent armor

- **Tool: Edge-on Impact (EOI) Method**

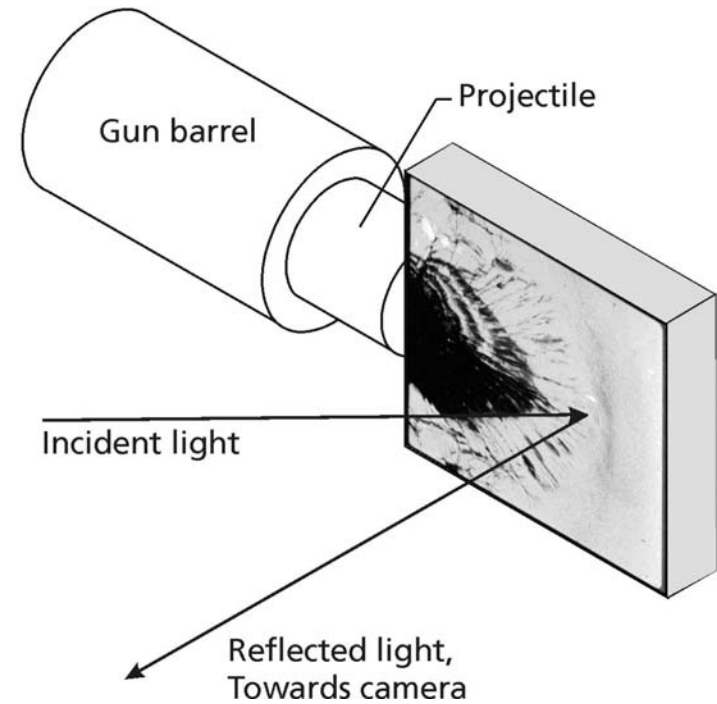
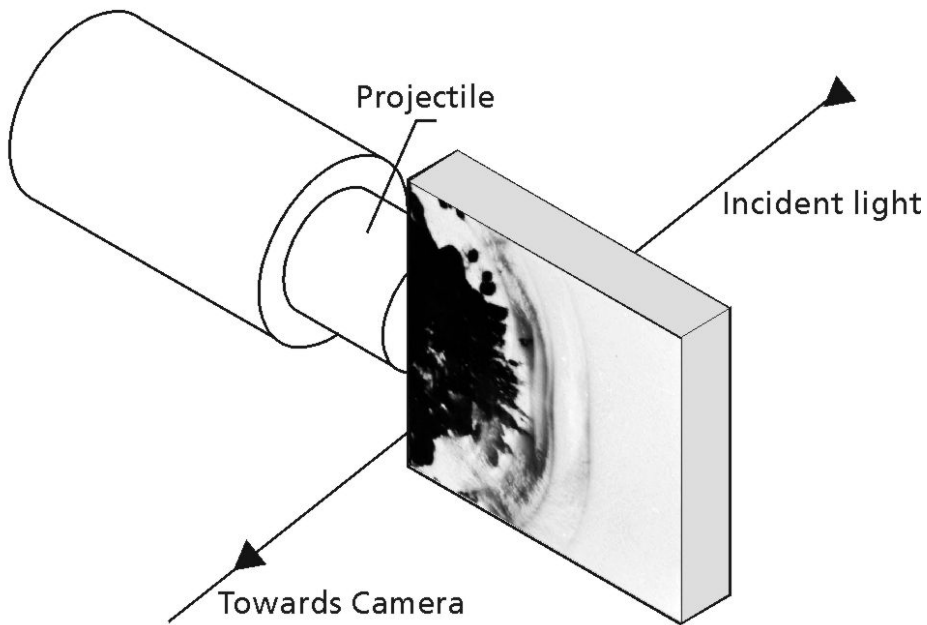
Visualization of damage evolution during the wave propagation phase and penetration

Characterization of materials by macroscopic fracture patterns, crack front velocities (damage velocities), single crack velocities

Test Set-up with 1 Cranz-Schardin Camera



Shadowgraph and reflected light set-up



Test Matrix Design

- Perform pairs of tests:

Visualization of damage

⇒ First test in regular **shadowgraph** arrangement

Visualization of Wave propagation

⇒ Second test at the same conditions with **crossed polarizers** arrangement

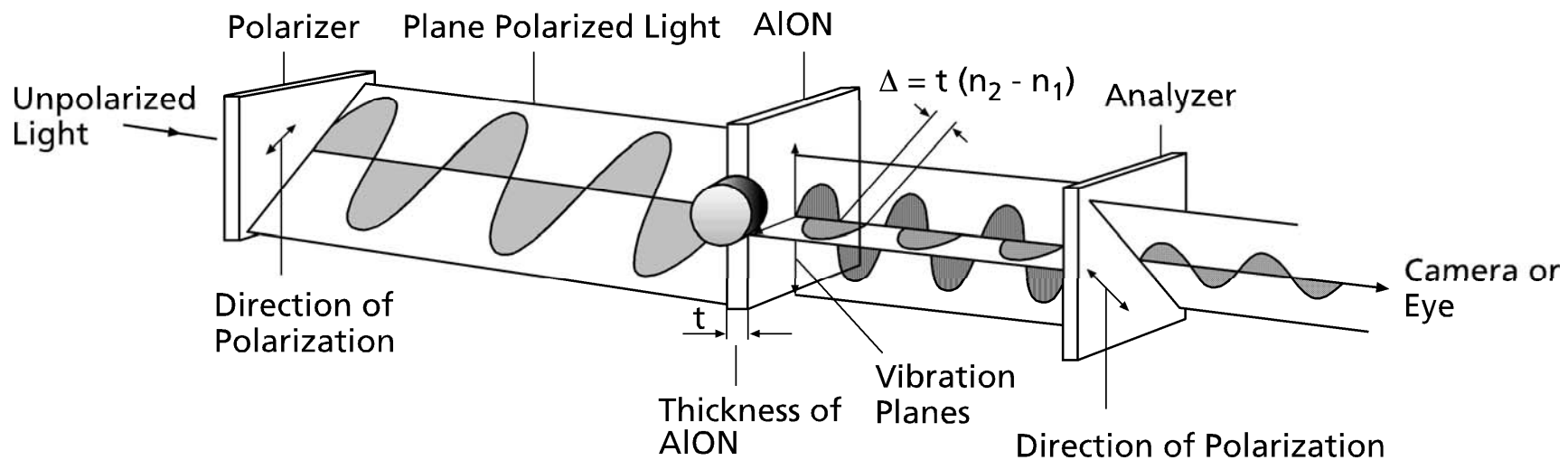
- **Phenomenology:** Nucleation of cracks, number, density
- Impact velocity range 250 m/s – 950 m/s

Photo-elastic Effect – Stress Induced Birefringence

- Material is getting optically anisotropic under mechanical loading

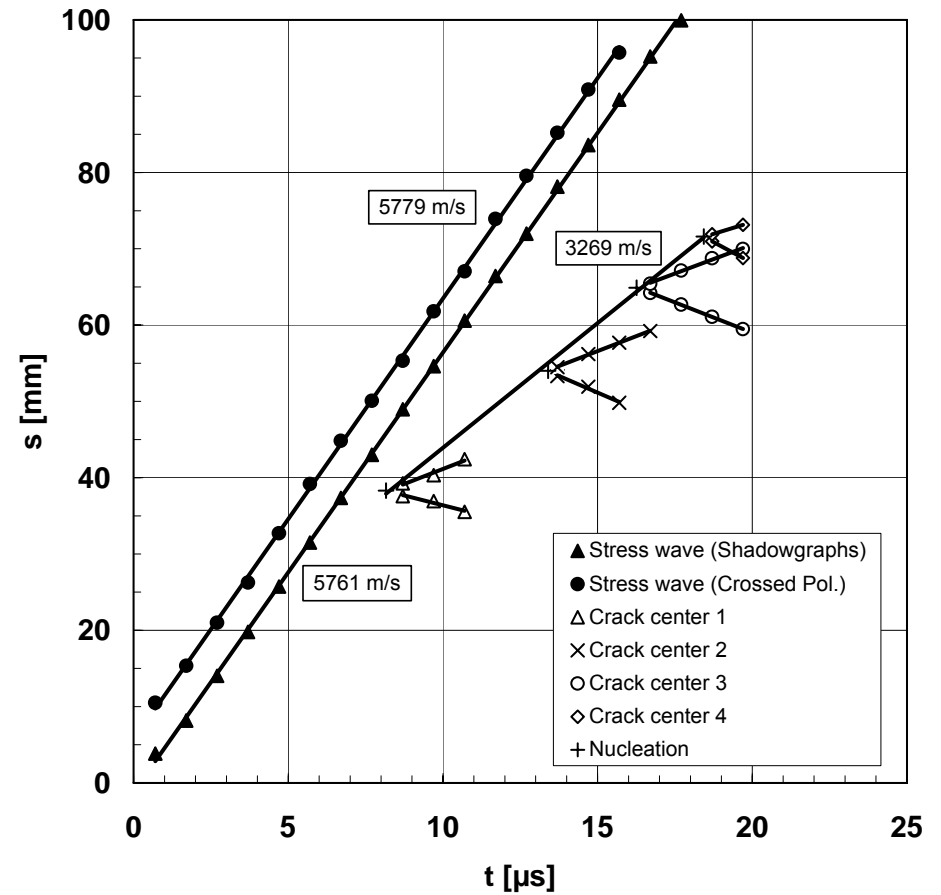
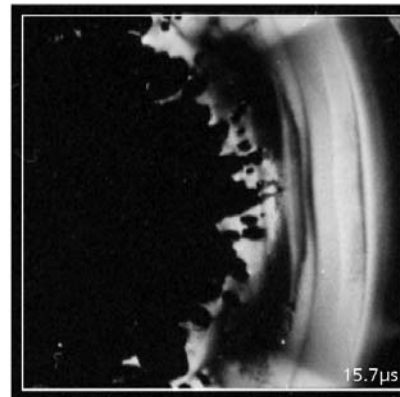
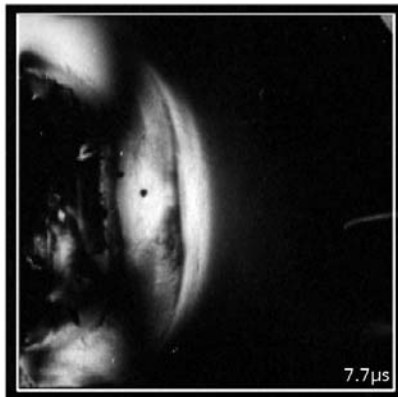
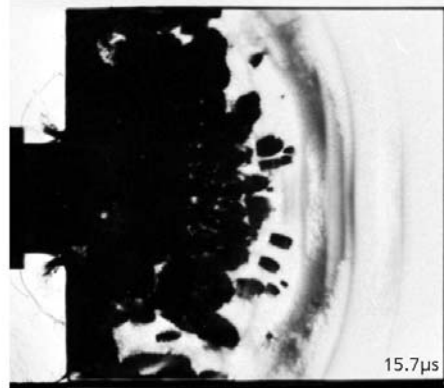
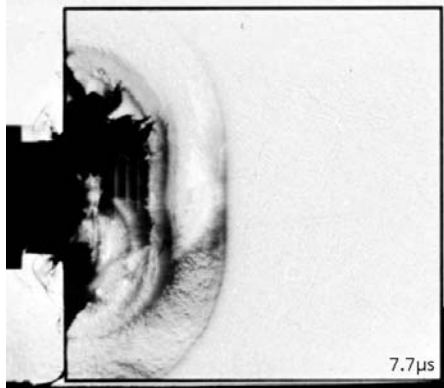
- Refractive indices: $\Delta n = (n_1 - n_2) = C_0 (\sigma_1 - \sigma_2)$

- Optical retardation: $\delta = (n_1 - n_2) \cdot t_p = C_0 \cdot (\sigma_1 - \sigma_2) \cdot t_p$



Baseline data with Starphire™ high purity soda-lime glass

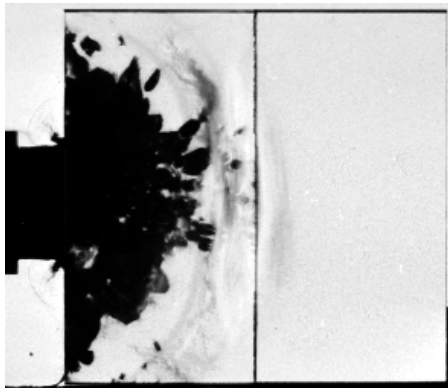
Plane Light



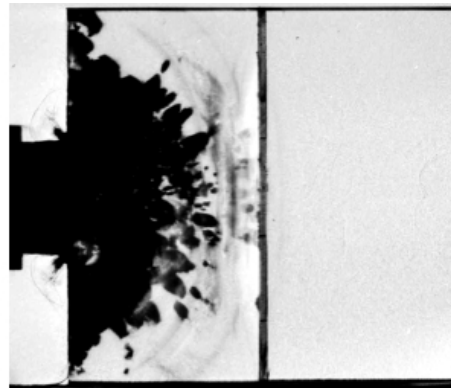
Crossed polarizers

Laminates with DF interlayers of different thickness after 10.7 μ s

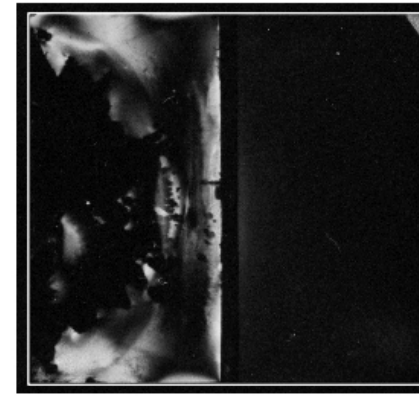
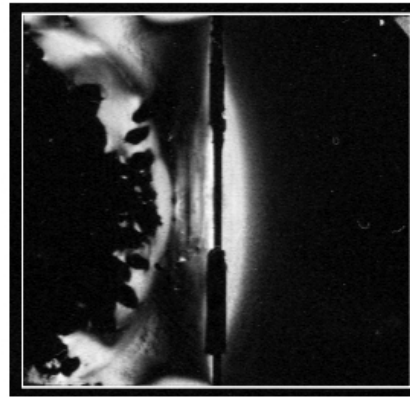
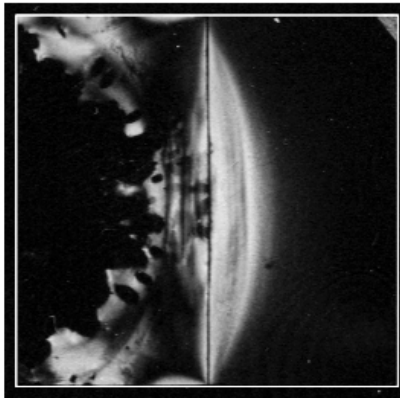
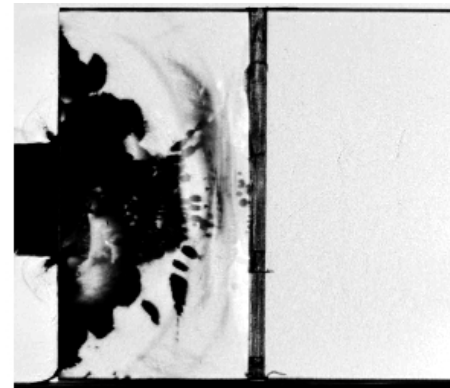
0.64 mm (0.025")



2.54 mm (0.100")



5.08 mm (0.200")

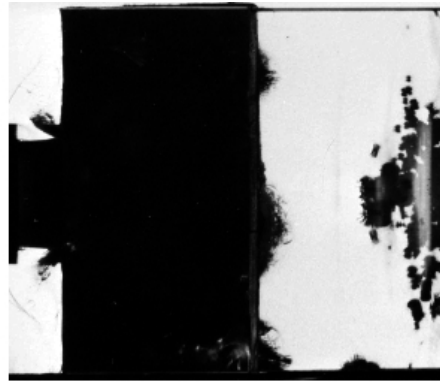


Laminates with DF interlayers of different thickness after 23.7 μ s

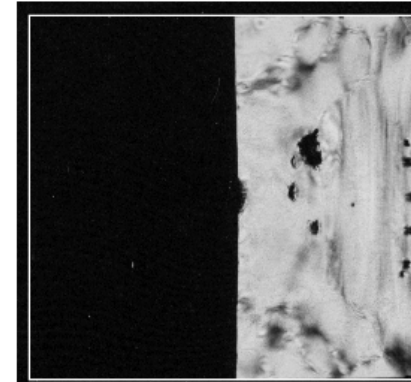
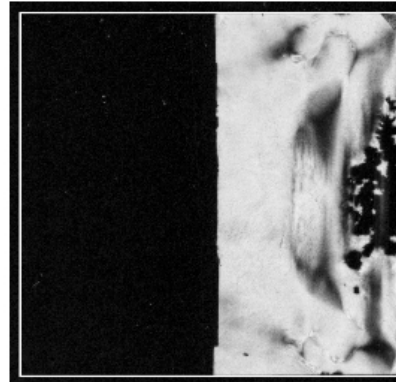
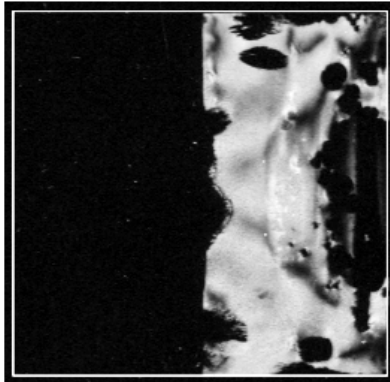
0.64 mm (0.025")



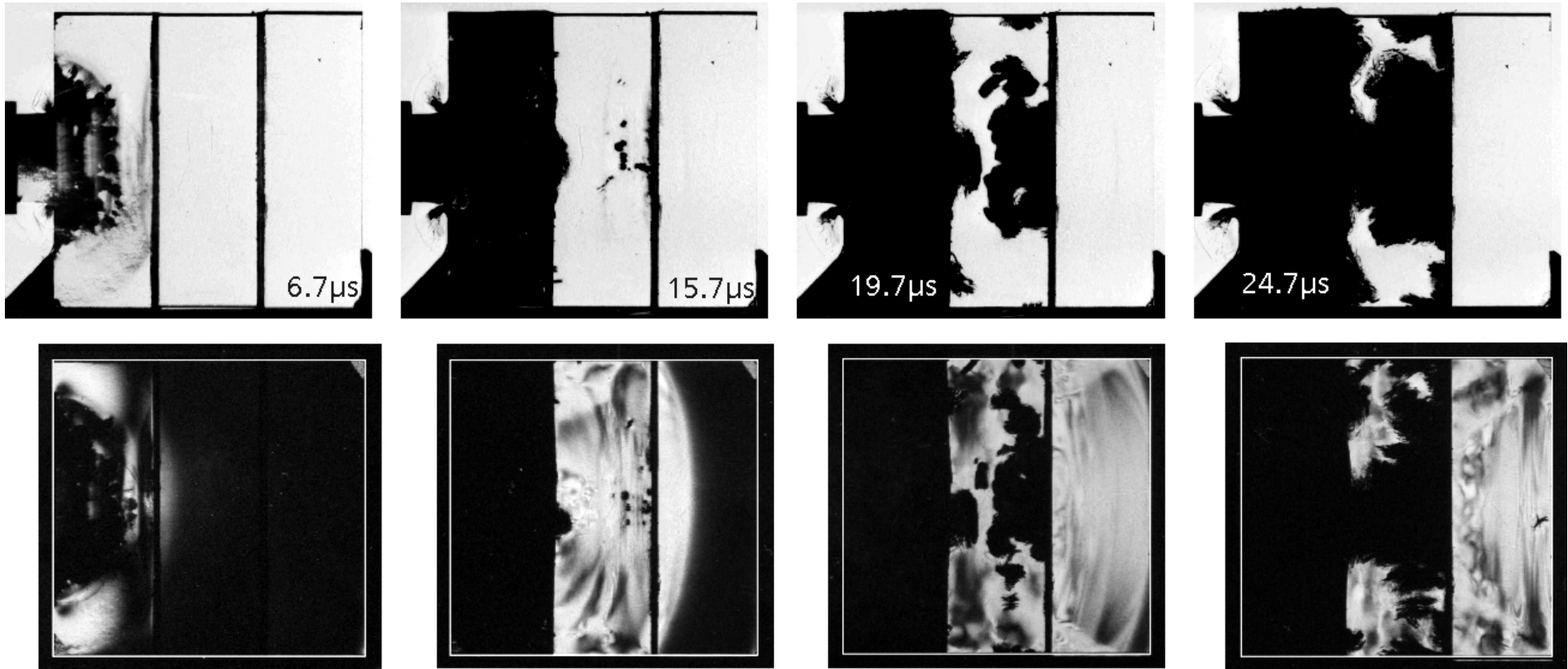
2.54 mm (0.100")



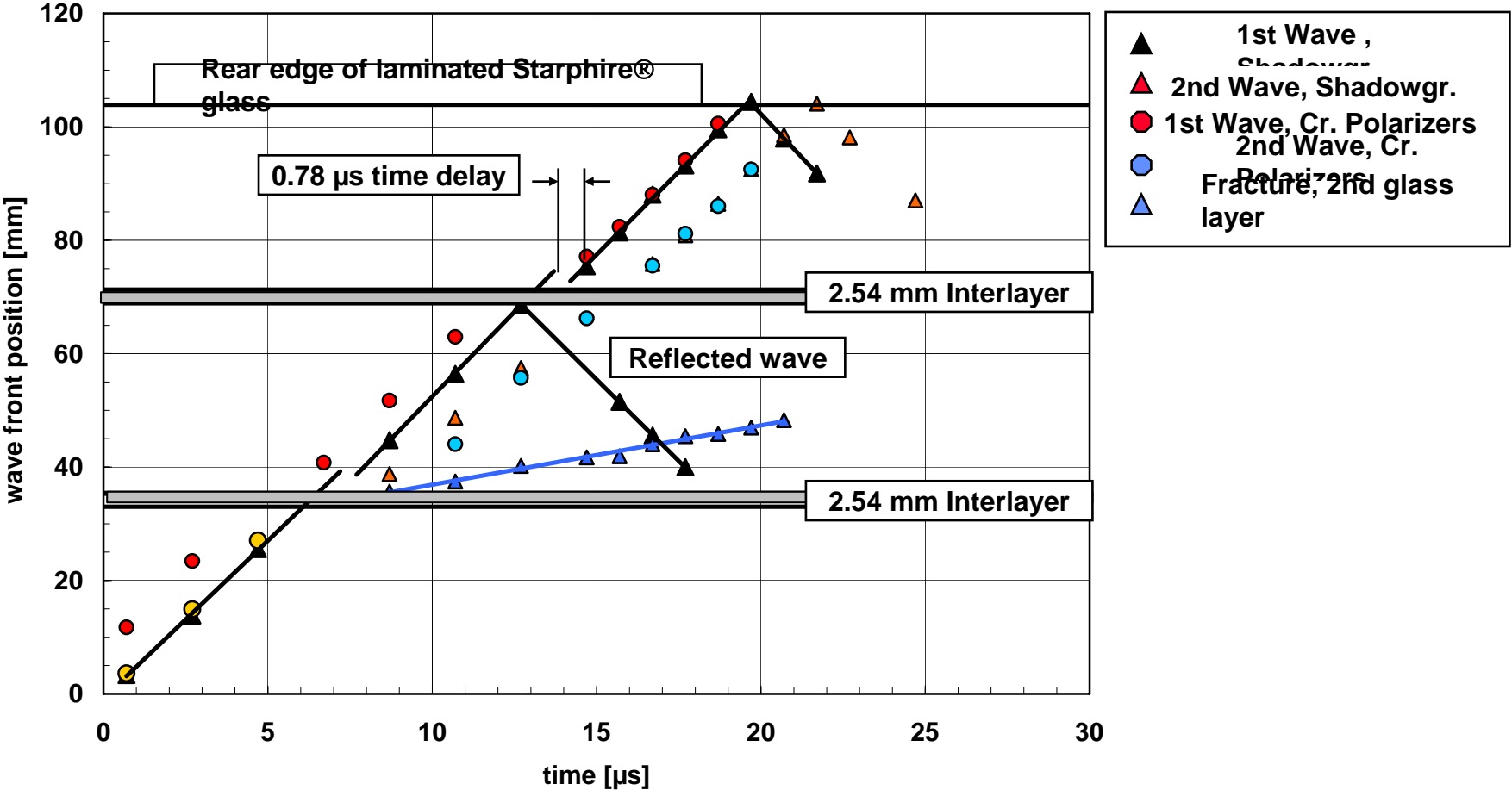
5.08 mm (0.200")



Three layer target: 2 x 2.54 mm DF Interlayer



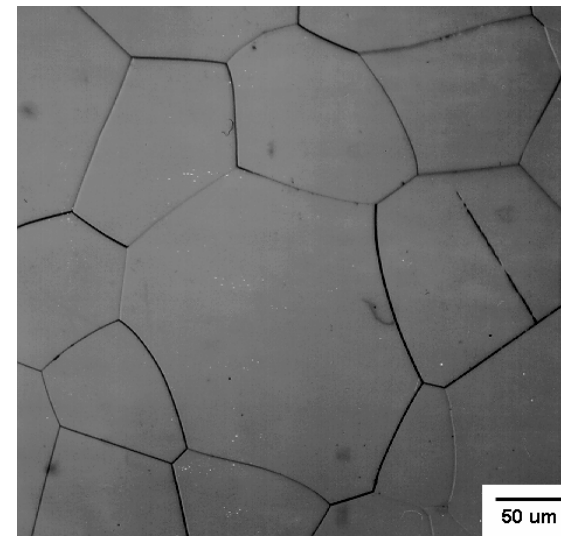
Path-time history of wave propagation in 3-layer target



Transparent polycrystalline ceramic AlON: Aluminum oxynitride ($9 \text{ Al}_2\text{O}_3 \cdot 5 \text{ AlN} - \text{Al}_{23}\text{O}_{27}\text{N}_5$)

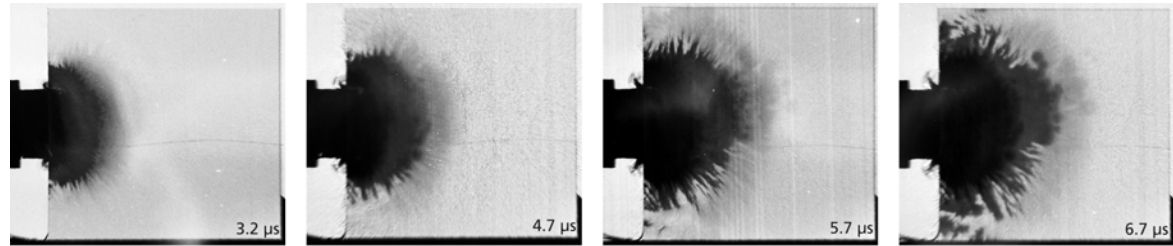
Material properties (Data Surmet)

Average grain size: 150 - 250 μm
Transmission: 83 % ($\lambda = 640 \text{ nm}$, 2 mm Thickness)
Hardness: 1800 ± 74 ($\text{HK}_{200\text{g}}$)

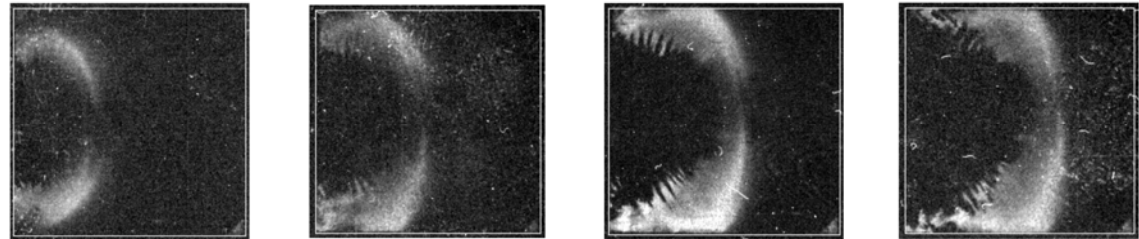


AION

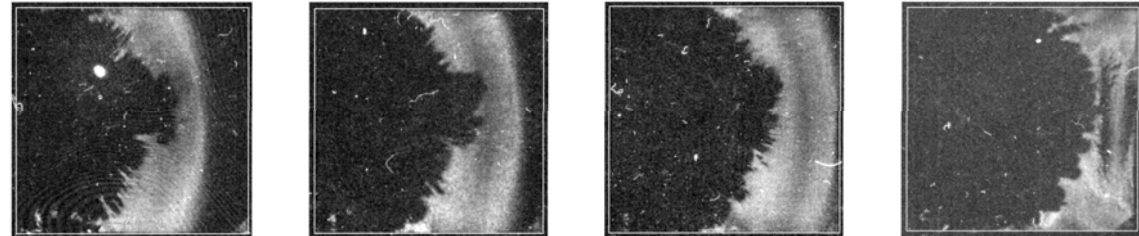
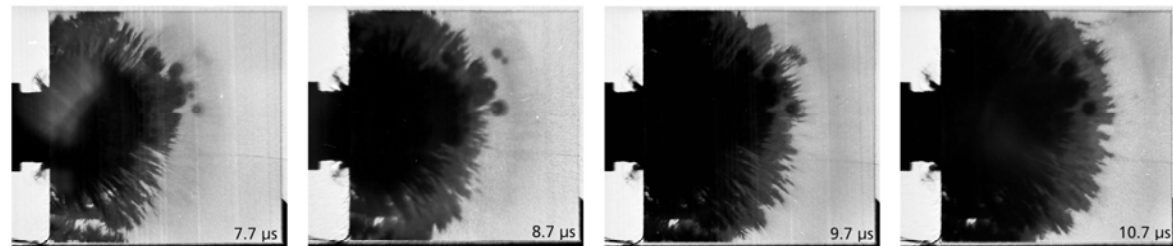
Plane light



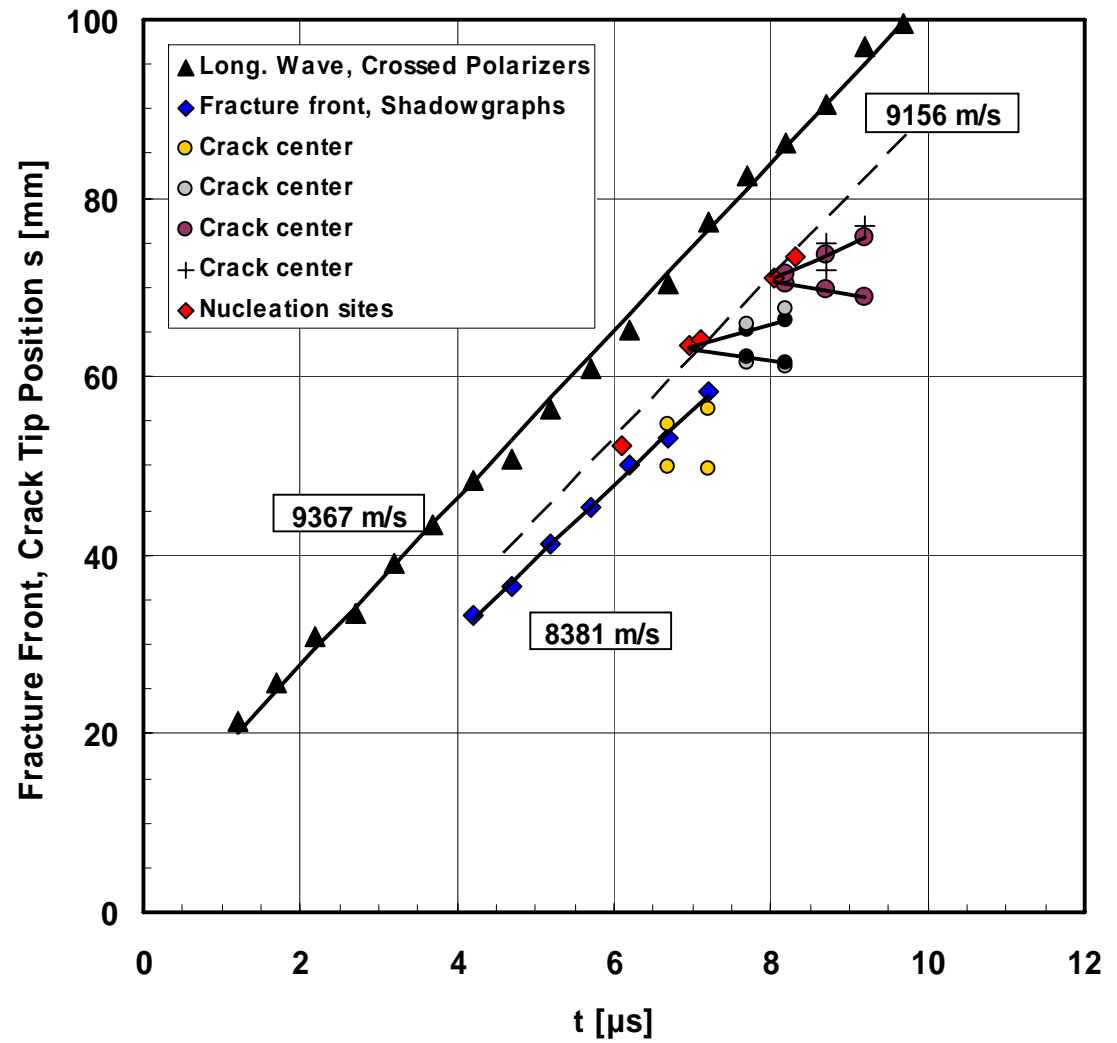
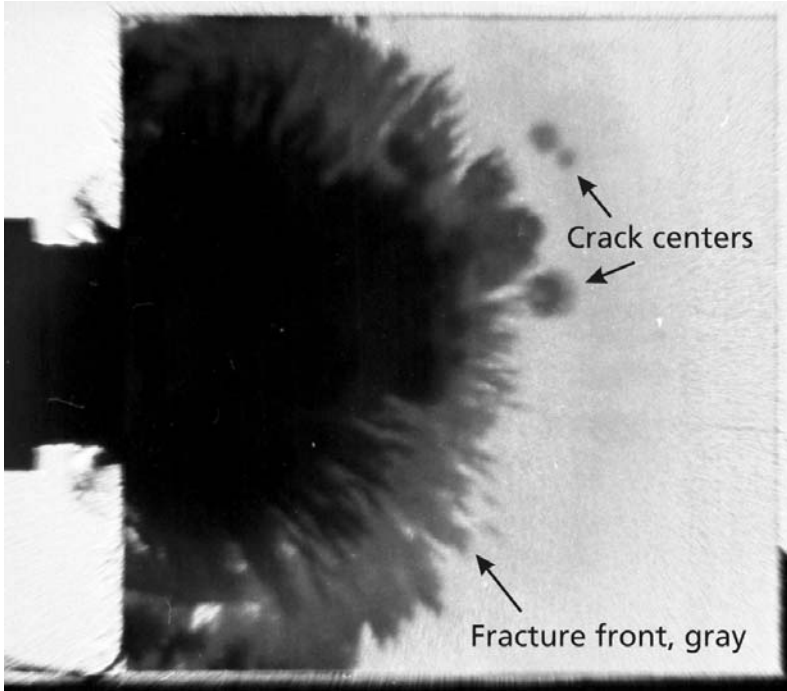
Crossed polarizers



Impact velocity ≈ 380 m/s

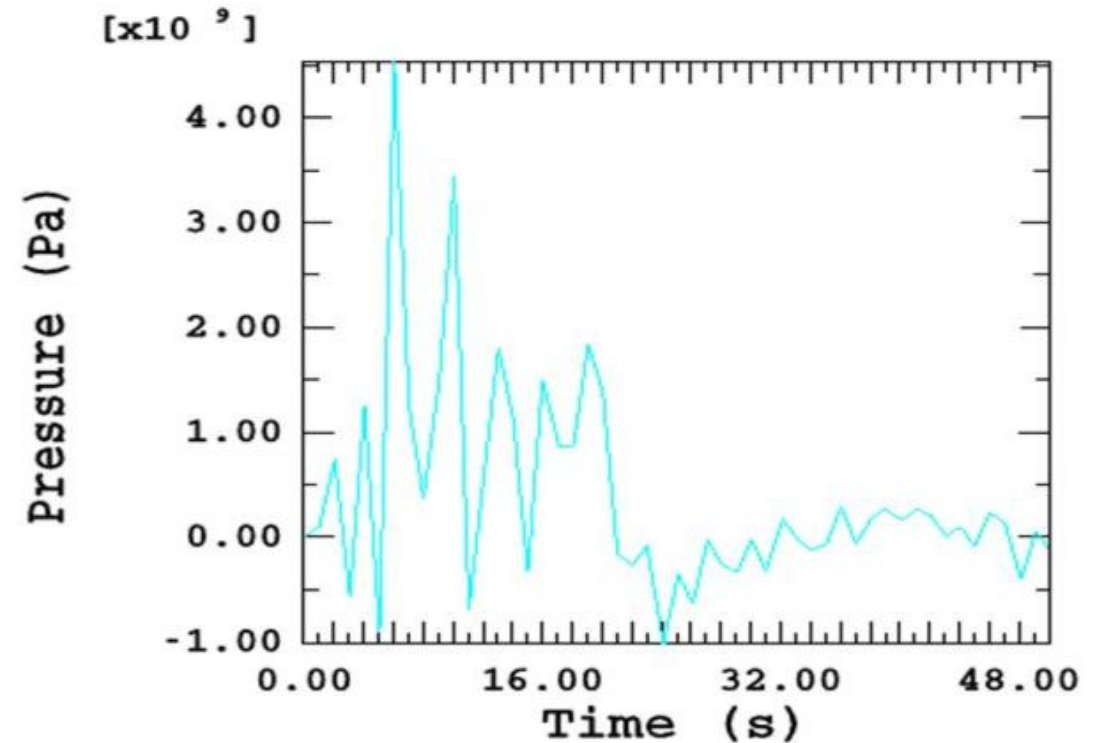
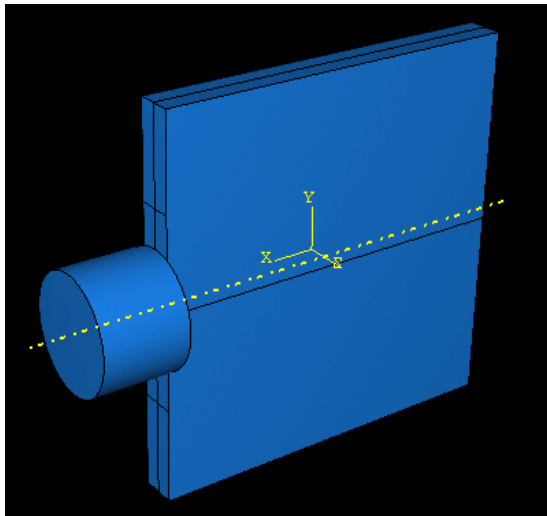


Path-time plot for tests at $v_p = 381/368$ m/s



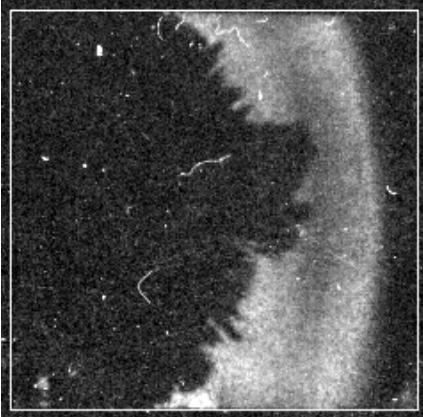
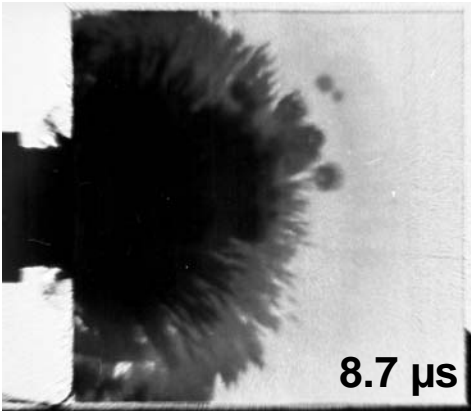
Stress wave simulation (Johns Hopkins University)

Pressure, monitored at impacted edge

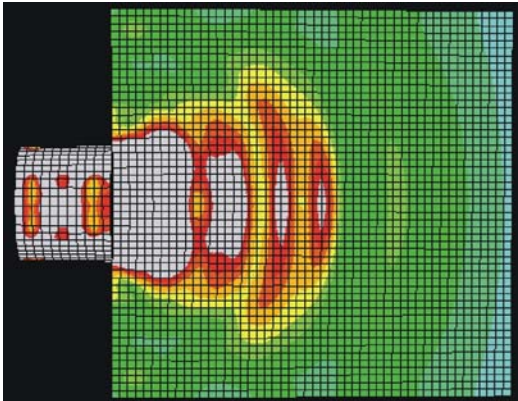


Elastic wave propagation (no damage)

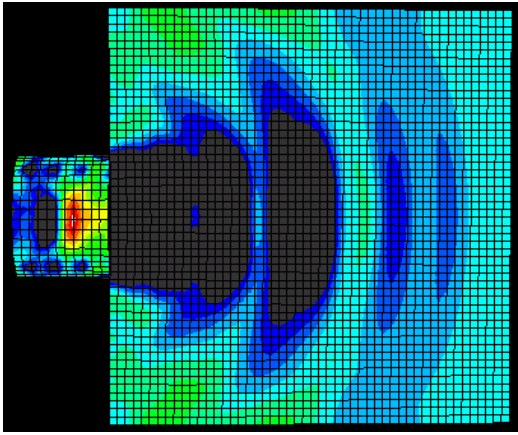
Experiment (EMI)



Simulation (JHU)



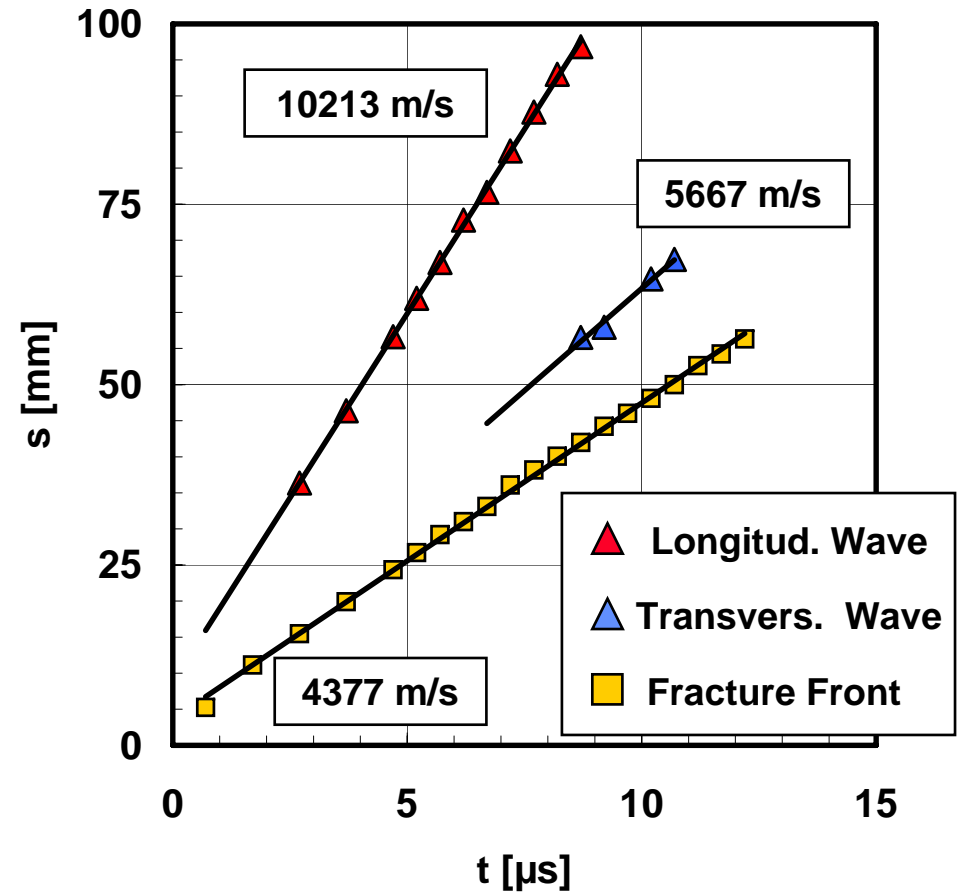
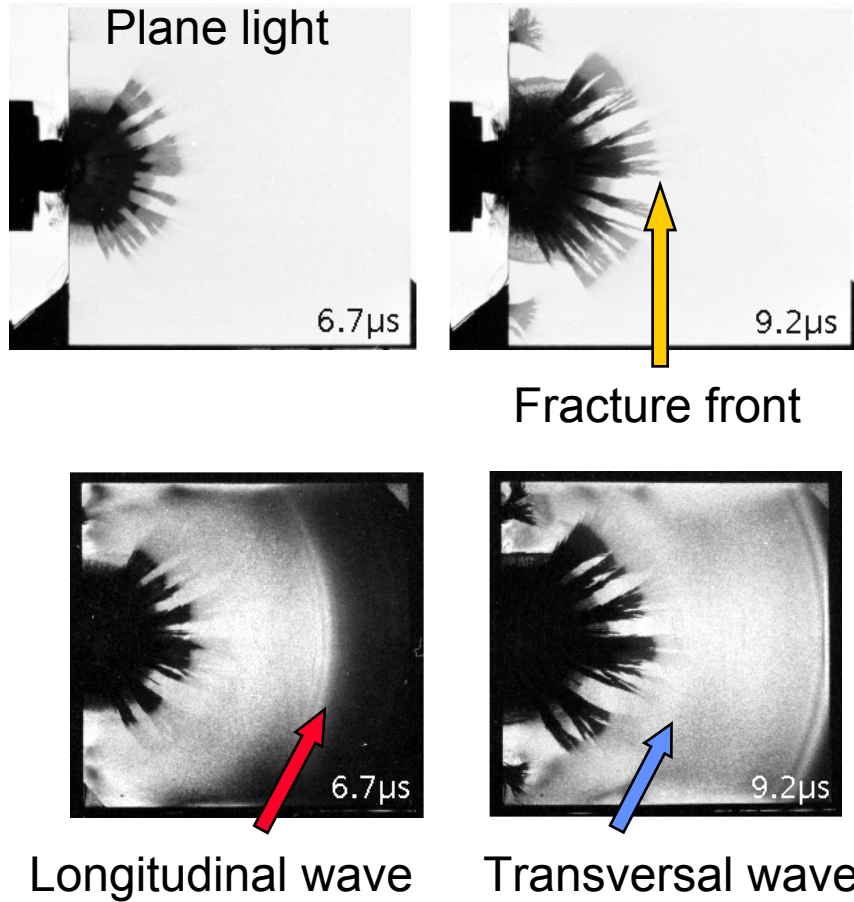
von Mises stress



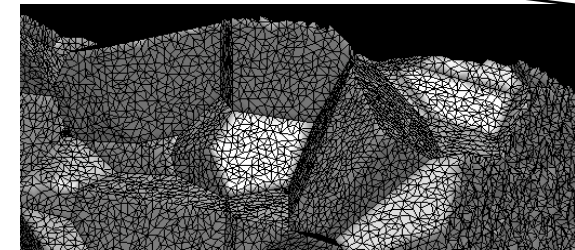
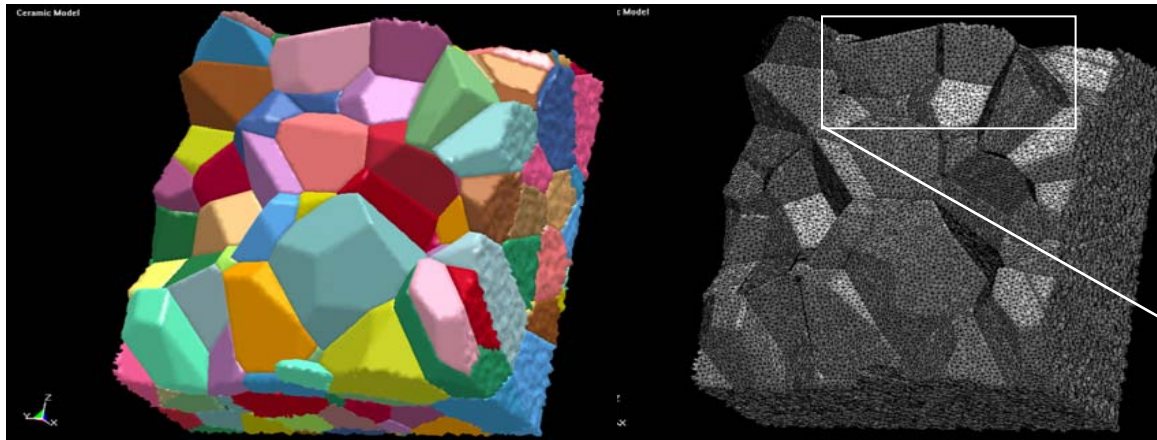
S11 stress

Principal axis

Steel Sphere -> AION, $v_p = 429/ 426$ m/s



EMI Modelling: Lattice Generation in 3D using Power Diagrams



Grains at the surface in 3D, meshed

Ceramic Model



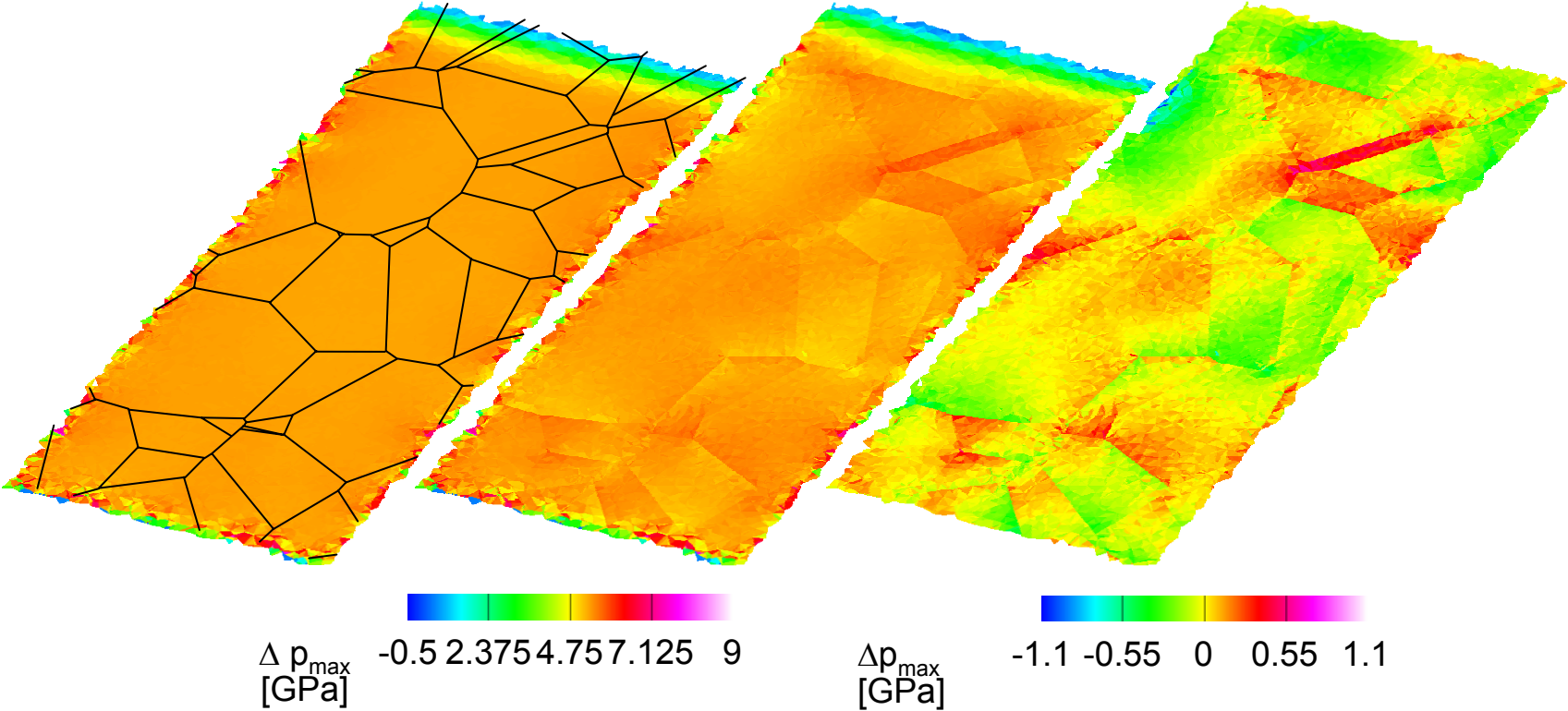
Left: Smooth virtual cut
Right: Smooth cut
preserving the rough
granular structure

Results: Isotropic vs. anisotropic material model

Isotropic

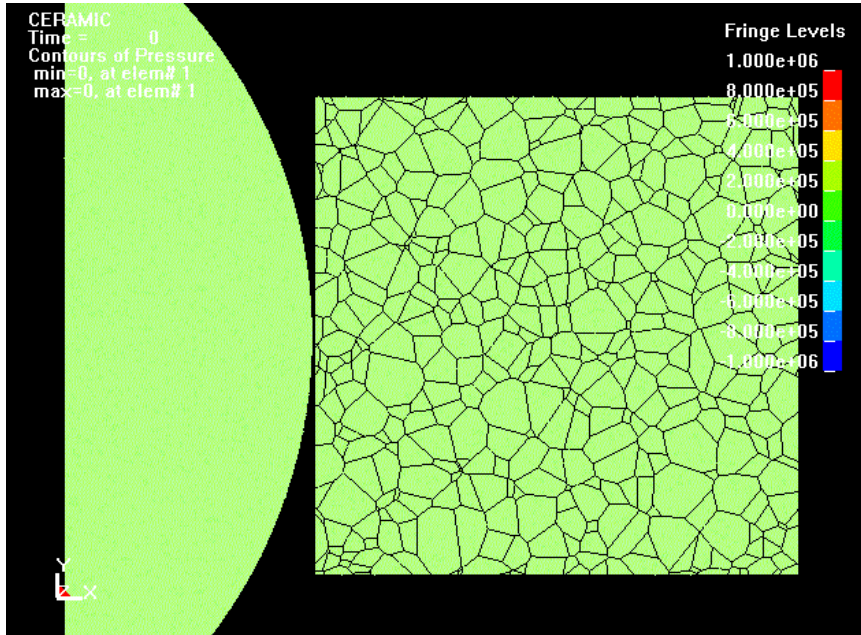
Anisotropic

Difference in pressure

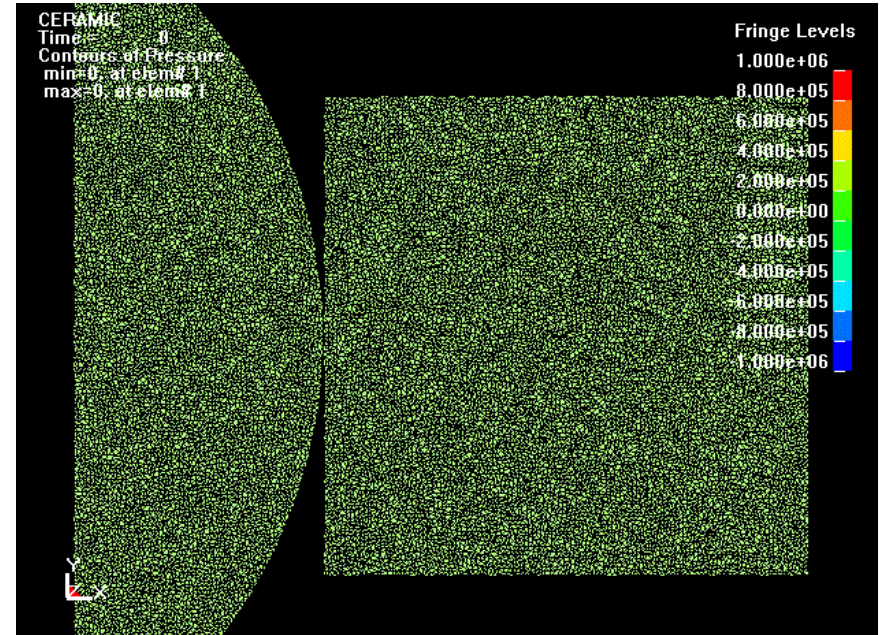


EOI Result: AION impacted by a steel sphere at 450 m/s

Grain structure



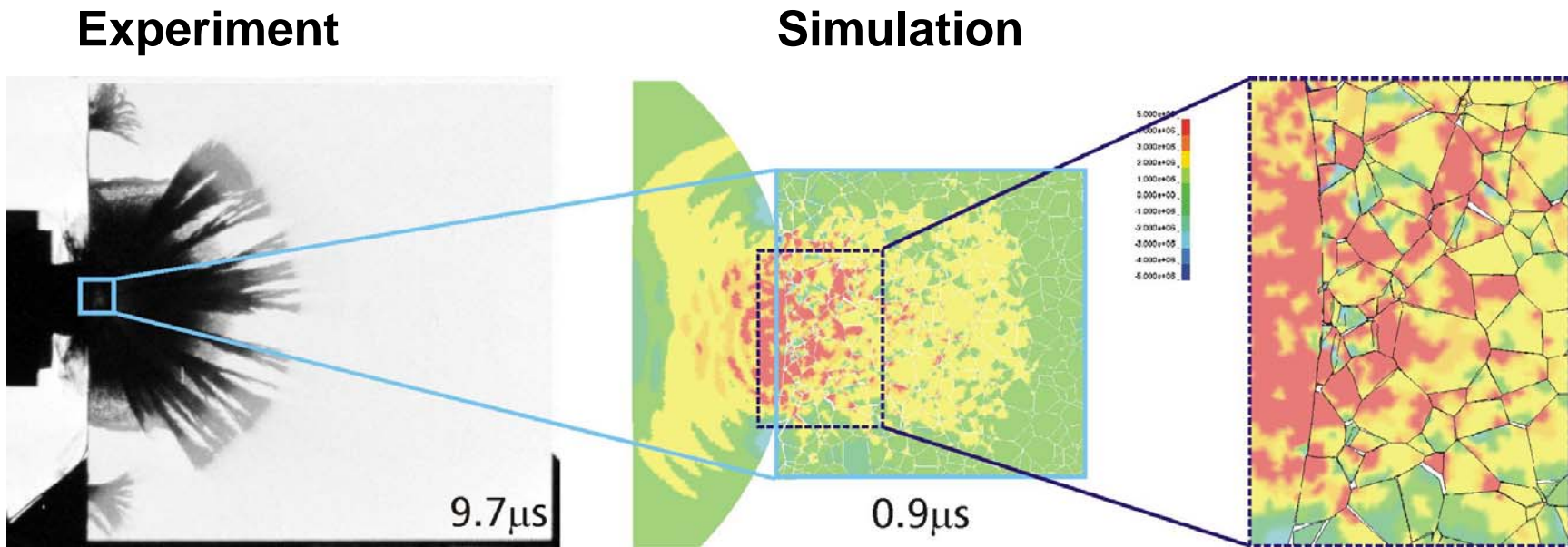
Mesh structure



Correct wave velocity ~ 10000 m/s
Correct fracture velocity ~ 4500 m/s

Limitation on the length scale

Limitations in length scale with using a finite elements approach, explicitly modelling the microstructure and failure



Summary

- Wave and damage propagation have been visualized in transparent armor materials by means of the Edge-on Impact test method.
- The influence of bonding layer thickness on damage evolution in Starphire glass laminates was examined.
- The high resolution of the high-speed photographs allows for the determination of stress wave time delay due to bonding layers.
- The polycrystalline microstructure of AlON was incorporated in a model and the formation of fracture was successfully modelled at EMI.